

# Virtual Mössbauer Spectrometer in the PXI Modular System

Jiri Pechousek and Miroslav Mashlan

Department of Experimental Physics, Palacky University, Olomouc, Czech Republic

**Abstract**— A virtual instrumentation programming method has been used for building a computer-based Mössbauer spectrometer. Data acquisition is realized via two PXI or PCI commercially available modules, the digital oscilloscope NI 5102 and the function generator NI 5401 (National Instruments), which are supported by relevant software drivers. Virtual Mössbauer spectrometer is implemented by the graphical programming language LabVIEW 7 Express. The RTSI bus is used for a synchronization of the registration of gamma ray photons with a relative velocity of the motion between the radioactive source and the sample. The amplitude selection of the impulses from the detector output is carried out by an assistance of the Waveform Peak Detection.vi function. The sampling rate of the detector output signal and frequency of the velocity signal determine the number of registration channels of the measured Mössbauer spectrum.

**Keywords**— Virtual instrument, PXI system, Mössbauer spectrometer, Peak detection.

## I. INTRODUCTION

Mössbauer spectroscopy, based on the phenomenon of recoilless nuclear emission and resonant adsorption of gamma rays, is a frequently used research tool in many areas of research such as physics, chemistry, biology, metallurgy etc.

Various computer techniques have been intensively used in their whole ranges for a design of Mössbauer spectrometers. In recent times, many designers have completed Mössbauer spectrometers in a configuration based on NIM [1,2], CAMAC [3,4], VME [5], and other modular systems. Some published designs of computer-based spectrometers have been solved in the form of computer plug-in boards [6,7], other spectrometers have used some commercially-available cards [8]. Different programming languages have been utilized for the software implementation of Mössbauer spectrometers. The use of the graphical programming language LabVIEW [9] in a Mössbauer spectrometer design is described in [10,11]. In these spectrometers, the LabVIEW programs are used only as a communication tool between the autonomous system and the computer via the serial port. However, only few advantages of LabVIEW data acquisition functions and libraries are used.

With the help of the new programming techniques and commercially available modules, a new type of the Mössbauer spectrometer has been built.

## II. SPECTROMETER DESCRIPTION

PXI standard (PCI eXtension for Instrumentation) combines high-speed PCI bus with integrated timing and triggering, specifically designed for measurement and automation applications. The function generator module NI 5401 and the digital oscilloscope module NI 5102 are used as a velocity generator and detector signal digitizer of the Mössbauer spectrometer, respectively.

NI 5102 module is an 8-bit dual-channel 20 MS/s digitizer with an input voltage range from  $\pm 50$  mV to  $\pm 5$  V. The NI 5102 uses a pair of 20 MS/s 8-bit flash ADCs, and the real-time sampling rate ranges from 20 MS/s down to 1 kS/s. Before being transferred into the host computer memory, data are recorded into the onboard acquisition memory. NI 5401 module is a full-featured 40 MS/s function generator. Analog voltages generated by a 12-bit DAC pass through a low-pass filter and amplification/attenuation scheme to maximize a dynamic range. The NI-SCOPE and NI-FGEN instrument driver are used in NI 5102 and NI 5401 applications. Both devices, including software support by the interactive Soft Front Panel, are available for the PXI and PCI standards [12].

### A. Spectrometer configuration

A block diagram of the novel computer-based modular spectrometer is shown in Fig. 1. There are two main parts; the first one is a computer with NI 5102 and NI 5401 modules controlled by VI (Virtual Instrument). Their synchronization is provided by a RTSI bus (Real Time System Integration; PXI Trigger consists of the RTSI bus and other special synchronization signals). The second part is a spectrometric bench which includes a feedback circuit for a movement control [10], transducer [13] with radioactive source, sample and detector of gamma rays with a high voltage power supply.

The spectrometric bench is shown in Fig. 2. The mini transducer, scintillation detector, source and absorber are placed in the metallic tube (diameter 65 mm, length 300

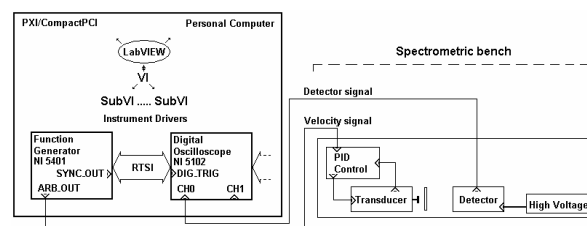


Figure 1. Block diagram of the Mössbauer spectrometer.

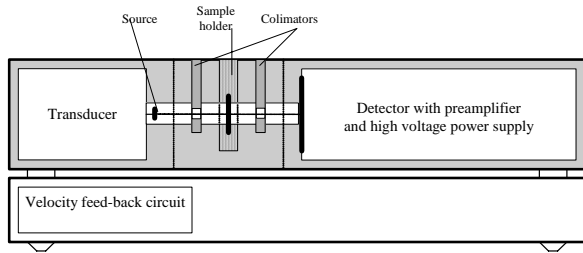


Figure 2. Spectrometric bench.

mm) on the mounting bench. A velocity feedback circuit is located at the base of the mounting bench.

The driving system consists of an electromechanical mini transducer [13], an electronic control system and a NI 5401 module. The mini transducer of the double-loudspeaker type is characterised by low dimensions (diameter 48 mm, length 62 mm) and low weight (360 g). The resonance frequency of mini transducer is about 35 Hz. The function generator NI 5401 generates a velocity signal at ARB OUT output. At SYNC OUT output, a trigger signal is available for a synchronization of other devices. In the case of our spectrometer, it is used for the synchronization between the signals coming from the gamma-ray detector and a generation of the velocity signal. The signals from the detector are directly connected to the CH0 input of the digital oscilloscope, which visualizes the final Mössbauer spectrum.

The software support of the presented spectrometer is divided into few SubVIs that are linked together to one VI in a given hierarchy. These SubVIs provide all core functions of the standard Mössbauer spectrometer.

**B. Signal processing**

The negative pulses from the photomultiplier tube with a NaI:Tl scintillation crystal are sampled by 5 MS/s sampling rate (see Fig. 3) so that their locations and magnitudes of their amplitudes are obtained.

The amplitude selection process is controlled by several input parameters of Waveform Peak Detection (WPKD) VI (see Fig. 4). This function finds the location, magnitude of amplitude and second derivative of the peaks in the detector signal. The Threshold and Width input parameters serve as separation tools of true detector pulses from the noise. The Threshold determinates the

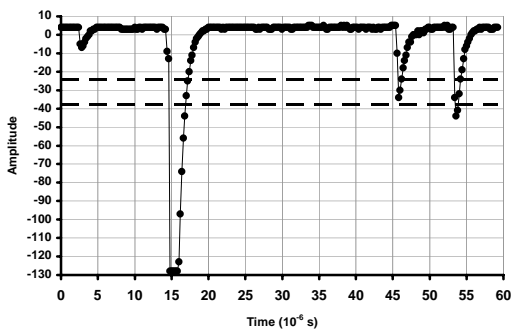


Figure 3. Sampled detector signal recorded from a <sup>57</sup>Co weak source.

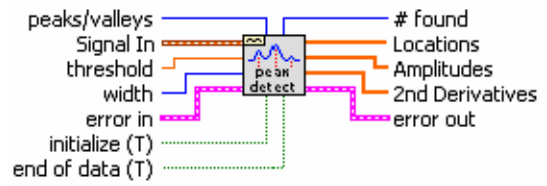


Figure 4. Icon of Waveform Peak Detection VI.

minimum value of the peak amplitude and the Width determinates the minimum peak width. The binary representation of the voltage detector signal is used; the voltage range of CH0 input is set up to 0.50 V (i.e.  $\pm 0.25$  V, which is represented by  $\pm 127$ ).

Subsequently, the amplitude values of the detection peaks, which WPKD VI produces, can be used for the multichannel amplitude analysis of the detector signal (see Fig. 5). The channel numbers correspond to the amplitudes of the impulses. As it is seen in Fig. 5, the amplitude spectrum consists of about 150 channels which is more than the maximum registered amplitude of 127. This is due to the fact that WPKD VI interpolates impulses, which results in higher amplitudes occurring in additional channels. On the other hand, the amplitude values of the detection peaks are used, together with the values on the Locations output of WPKD VI, for an accumulation of Mössbauer spectra. The value of the amplitude from WPKD VI is compared with low and high discrimination levels to find impulses corresponding to the 14.4 keV resonant Mössbauer photons (dashed lines in Fig. 3). The Locations output contains positions of valid peaks found in the current block of data. Evidently, the number of channels of the Mössbauer spectrum is determined by a sampling rate and frequency of the velocity signal, where the sampling rate depends on a type of the detector and the frequency of the velocity signal is given by transducer properties.

The synchronization between the relative movement of the source vs. sample and corresponding acquired signals from the detector uses the SYNC OUT signal, mounted on the RTSI bus, and pretriggered acquisition mode (see Fig. 6) [12].

The simplified scheme describing the algorithm of a Mössbauer spectrum collection is depicted in Fig. 7.

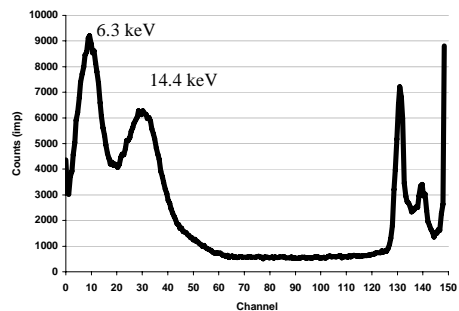


Figure 5. Amplitude spectrum of a <sup>57</sup>Co source.

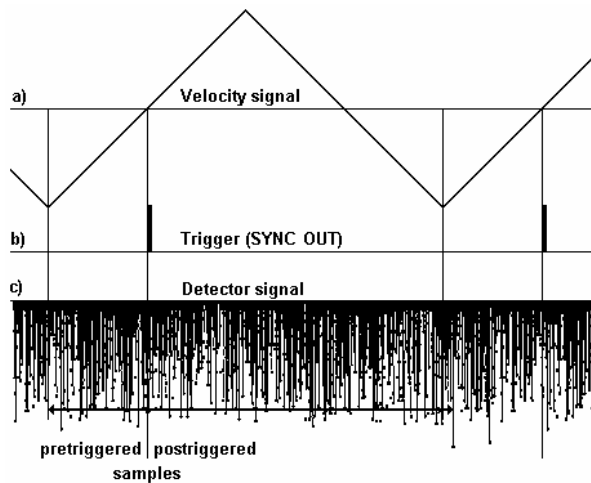


Figure 6. Synchronization between the velocity of relative movement of the source vs. sample and the detector signal registration.

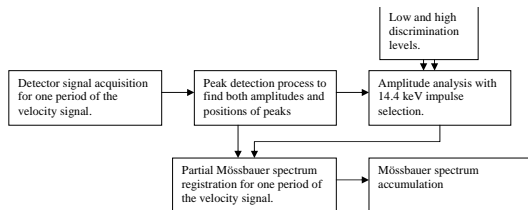


Figure 7. Algorithm of the Mössbauer spectrum accumulation.

With the help of low and high discrimination levels, the 14.4 keV selection window is set up. If the analyzed peak has an amplitude in the set range, number +1 is added to the correct channel whose number is given at the Locations output of WPKD VI. Based on the described principle of data selection, the Mössbauer spectrometer with sampling time axis has been built.

Thus, if the frequency of the velocity signal is set up to 20 Hz, the sampling process with a sampling rate of 5 MS/s results in 250 000 patterns of detector signal per one velocity period. There are then 250 000 potential locations and this value represents the number of velocity channels in the Mössbauer spectrum. This spectrum is also collected in 250 000 channels. For illustration, the measured Mössbauer spectrum of the standard hematite sample is shown in Fig. 8.

The next step is to fold the mirror records registered during the increasing and decreasing part of the velocity signal. In order to do so, it is necessary to find the channel number (index) which cuts the spectrum pattern into two



Figure 8. Measured Mössbauer spectrum of the standard hematite sample.

half-patterns. This is achieved by measuring the standard sample with a singlet spectrum (see Fig. 9). The resonance effect is programmatically computed for an interval of possible indexes, which aims at finding the appropriate index corresponding to a maximum resonance effect. The calculated index is then used for all measurements together with other constant parameters such as the frequency of the velocity signal, the sampling rate and the number of samples per one period of the move. The amplitude of the velocity signal can be changed, which means that the interval of possible velocities is variable. This allows the user to set other velocity range without any extra process of index searching.

The number of 250 000 velocity channels is unserviceable for subsequent mathematical processing. Hence, the number of channels is reduced by grouping the surrounding channels. As an example, the folded and reduced Mössbauer spectrum of hematite is presented in Fig. 10. The number of channels in the Mössbauer spectrum was optimized as follows. We measured the Mössbauer spectra for three frequencies of the velocity signal (15, 20, and 25 Hz). The spectra were recorded with a maximum number of channels. For each frequency, a test singlet spectrum was measured with the same background. After folding the mirror spectra, the velocity channels are grouped into sets, usually consisting of 128 channels. The contents of all 128 channels in one set are added up and this sum then creates one velocity channel of consecutively mathematically processed Mössbauer spectrum, which thus consists of 971 velocity channels. The grouping of 128 channels to one velocity channel

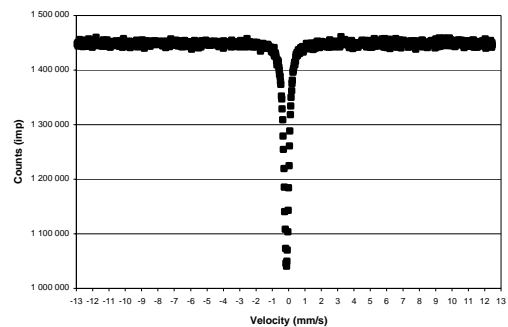


Figure 9. Standard singlet spectrum (after folding and reducing the number of channels).

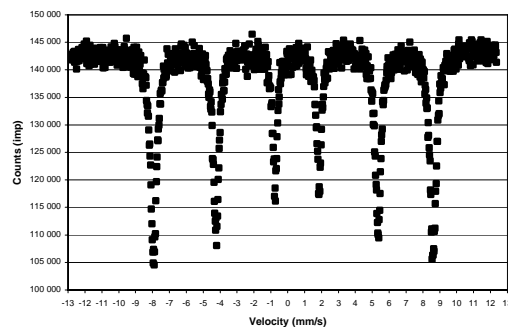


Figure 10. Spectrum of the standard hematite sample measured for 1 h (after folding and reducing the number of channels).

makes further mathematical processing of recorded Mössbauer spectrum more feasible. The results of the optimization process are demonstrated in Fig. 11 and Fig. 12 and are discussed in detail in the next section.

III. RESULTS AND DISCUSSION

The Mössbauer spectra collected for various frequencies of the velocity signal and with the maximum number of channels were grouped into consecutive sets consisting of 2, 4, 8, 16, 32, 64, 128, 256, 512, 1024, and 2048 channels after folding. This process resulted in Mössbauer spectra with different number of velocity channels. Each spectrum was fitted by a Lorentz function with a  $\chi^2$  minimalization. As-computed parameters were then used for the search of the optimal number of velocity channels of the spectrum in real measurements. Fig. 11 and Fig. 12 show dependences of computed probability of correspondence between the theoretical (Lorentz) and experimental shape of the spectral line, and resonance effect vs. number of channels, respectively. Fig. 11 demonstrates the decrease of the probability of correspondence between theoretical and experimental line shape for a number of channels being less than 1 000. Fig. 12 shows the plateau of constant resonance effect occurring for the number of channels being in the range from about 500 to 10 000.

It is obvious that minimum optimal number of channels in Mössbauer spectrum, when the resonance effect does not decrease and the fitting process is correct with the Lorentz function, is about 1 000. In general, grouping to

the sets containing 128 channels is close to optimum.

Table 1 summarizes the results of the Mössbauer measurements with a standard sample. In this table, the Channels column shows the optimum number of velocity channels in resulted spectrum and the last three columns represent the results of the fitting procedure with Lorentz curve.

The main parameter characterizing the quality of the Mössbauer spectrometer (particularly its driving system) is the nonlinearity of the velocity scale. Three enriched  $\alpha$ -Fe<sub>2</sub>O<sub>3</sub> Mössbauer spectra were collected with a NaI:Tl scintillation detector in order to evaluate the nonlinearity of the velocity scale for each frequency (15, 20, and 25 Hz). The spectrometer was assembled with a mini transducer [13] and a <sup>57</sup>Co(Cr) source with an activity of 20 mCi was used. Experimental positions of lines,  $x(i)$ , and their nonlinearities,  $non(i)$ , are shown in Table 2.

The spectral lines of the Mössbauer spectrum were approximated by the Lorentz functions. The least square method was used for fitting the experimental positions of the spectral lines to its theoretical positions and the nonlinearity for all line positions were then calculated by the equation of the form [13]

$$non(i) = \frac{x(i) - a \cdot v(i) - b}{v(6) - v(1)}$$

where  $i$  ( $i = 1$  to  $6$ ) is a line number,  $x(i)$  represents the experimental position of the line,  $v(i)$  denotes the theoretical position of the line and  $a$ ,  $b$  stand for the parameters calculated from the least square method.

It is obvious that positions, nonlinearities and line widths (FWHM) of Mössbauer spectral lines are approximately the same for all frequencies.

IV. CONCLUSION

An autonomous computer-based system for Mössbauer spectroscopy has been designed which uses all advantages of computer techniques and new programming methods. This system allows programming the number of channels, frequency and amplitude of the velocity of the relative movement between radioactive source and sample, the time for data acquisition and their storage, displaying and analysis. The spectrometer (software) can be adapted for various geometry measurements and there is no problem to implement the algorithms for main measuring modes (i.e. constant and variable velocity modes) and amplitude analysis. The control of this system is simple and easy; moreover, the operator interface is very friendly for the user (see Figs. 13 and 14). In addition, using the standard commercially available cards, the novel equipment significantly improves its fidelity. Since data acquisition cards are controlled by software (firm instrument drivers), it is easy to change its way of operation according to other experimental requirements. Thus, a flexible and expandable Mössbauer spectrometer system has been built.

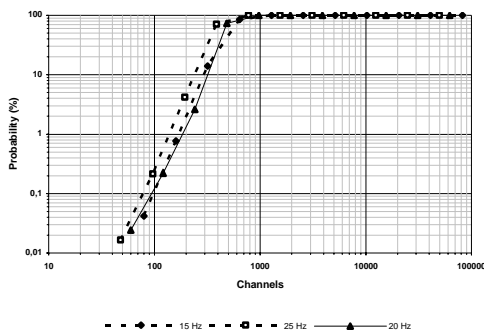


Figure 11. Probability of correspondence between theoretical and experimental line shape vs. number of channels.

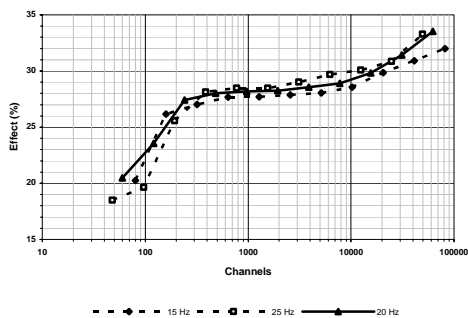


Figure 12. Magnitude of resonance effect vs. number channels.

TABLE I. RESULTS OF THE MEASUREMENTS.

Frequency (Hz)	Channels	Background	Resonance effect (%)	Collection time (hh:mm)	Line's position (mm/s)	FWHM (mm/s)	$\chi^2$
15	1 282	1 370 000	27.7	20:00	-0.099	0.333	43.3
20	971	1 450 000	28.2	16:25	-0.100	0.336	44.3
25	776	1 470 000	28.5	13:25	-0.100	0.334	33.2

TABLE II. RESULTS OF THE NONLINEARITY MEASUREMENTS.

Frequency (Hz)	i		1	2	3	4	5	6
15	$x(i)$	(mm/s)	-8.070	-4.351	-0.831	1.802	5.324	8.623
	non(i)	(%)	0.14	-0.11	-0.06	-0.03	-0.02	0.09
	FWHM	(mm/s)	0.425	0.383	0.330	0.324	0.379	0.430
20	$x(i)$	(mm/s)	-8.075	-4.349	-0.828	1.812	5.324	8.618
	non(i)	(%)	0.11	-0.10	-0.05	0.02	-0.02	0.05
	FWHM	(mm/s)	0.425	0.395	0.321	0.359	0.388	0.439
25	$x(i)$	(mm/s)	-8.072	-4.347	-0.834	1.806	5.327	8.621
	non(i)	(%)	0.12	-0.09	-0.08	-0.01	-0.01	0.07
	FWHM	(mm/s)	0.419	0.366	0.322	0.310	0.370	0.410
Standard	$v(i)$	(mm/s)	-8.090	-4.330	-0.818	1.810	5.330	8.610

ACKNOWLEDGMENT

Financial support from The Ministry of Education, Youth and Sports under project of research center No 1M6198959201 is gratefully acknowledged.

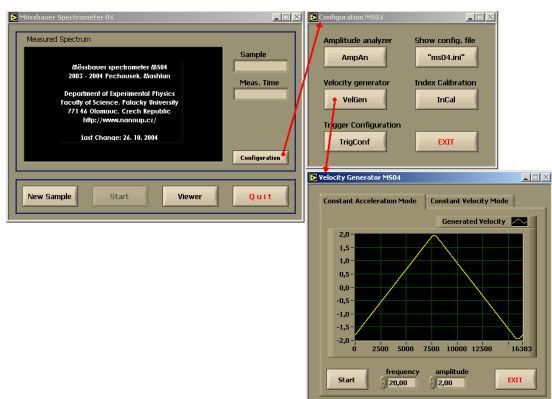


Figure 13. Main VI with a few SubVIs.



Figure 14. The set-up of the presented Mössbauer spectrometer.

REFERENCES

- [1] C. Verrastro, G. Trombetta, A. Pita, C. Saragovi, and S. Duhalde, "5nsec dead time multichannel scaling system for Mössbauer spectrometer," *Hyperfine Interact.*, vol. 67, 1991, pp. 689–694.
- [2] C. Verrastro, G. Trombetta, A. Pita, C. Saragovi, and S. Duhalde, "Zero dead time multichannel scaling system," *Nucl. Instrum. Meth. B*, vol. 73, 1993, pp. 425–428.
- [3] J. de Blois, "A memory module for experimental data handling," *Nucl. Instrum. Meth. A*, vol. 234, 1985, pp. 498–504.
- [4] S. V. Dudin, O. V. Ignatyev, and A. D. Pulin, "A fast signal processor for NaI(Tl) detectors," *Nucl. Instrum. Meth.*, vol. 352, 1995, pp. 610–613.
- [5] J. de Blois, A. J. H. Beunes, E. Boellaard, A. M. van der Kraan, E. A. Osterholt, et al., "A single-board VME mössbauer-spectrometry module," *Nucl. Instrum. Meth. B*, vol. 142, 1998, pp. 173–190.
- [6] D. Zak, M. Maslan, A. L. Kholmetskii, V. A. Evdokimov, A. R. Lopatik, et al. "Mössbauer spectrometer based on personal computer equipped with the YAlO<sub>3</sub>:Ce scintillation crystal," *Acta Phys. Slovaca*, vol. 45, 1995, pp. 85–88.
- [7] M. Maslan, D. Zak, A. Cholmeckij, V. Evdokimov, O. Misevich, et al., "The PC-AT based Mössbauer spectrometer," *Acta UPO, Fac. Rer. Nat. Physica XXXIII*, vol. 116, 1994, pp. 9–19.
- [8] G. Faigel, P. E. Haustein, and D. P. Siddons, "An IBM PC based Mössbauer spectrometer and data analysis system," *Nucl. Instrum. Meth. B*, vol. 17, 1986, pp. 363–367.
- [9] *LabVIEW 7 Express, User Manual*, National Instruments, National Instruments Corp., 2003.
- [10] M. Mashlan, D. Jancik, D. Zak, F. Dufka, V. Snasel, et al., "The Mössbauer spectrometer as a virtual instrument," in *Mössbauer Spectroscopy in Materials Science*, M. Miglierini and D. Petridis, Eds. Dordrecht: Kluwer Academic Publishers, 1999, pp. 399–406.
- [11] A. L. Morales, J. Zuluaga, A. Cely, and J. Tobón, "Autonomous system design for Mössbauer spectra acquisition," *Hyperfine Interact.*, vol. 134, 2001, pp. 167–170.
- [12] *The Measurement and Automation Catalog 2004*, National Instruments, National Instruments Corp., 2003.
- [13] V. A. Evdokimov, M. Mashlan, D. Zak, A. A. Fyodorov, A. L. Kholmetskii, et al., "Mini and micro transducers for Mössbauer spectroscopy," *Nucl. Instrum. Meth. B*, vol. 95, 1995, pp. 278–280.

AUTHORS

**J. Pechousek** is with the Department of Experimental Physics, Palacky University, Svobody 26, Olomouc 77146, Czech Republic (e-mail: [pechous@prfnw.upol.cz](mailto:pechous@prfnw.upol.cz)).

**M. Mashlan** is with the Department of Experimental Physics, Palacky University, Svobody 26, Olomouc

77146, Czech Republic (e-mail: [miroslav.maslan@upol.cz](mailto:miroslav.maslan@upol.cz)).

Manuscript received September 8, 2005. This work was supported in part by the U.S. Department of Commerce under Grant BS123456 (sponsor and financial support acknowledgment goes here).